The role of the hot-electron distribution function in the stability of the ELMO Bumpy Torus

K. Nguyen and T. Kammash
The University of Michigan, Ann Arbor, Michigan 48109

(Received 10 August 1982; accepted 20 May 1983)

Several recent studies of ELMO Bumpy Torus (EBT) stability show that conflicting results can emerge when different distribution functions for the hot-electron component are used. In this paper the role of the distribution function is established by examining the stability of various modes with the aid of two models. In the "slab" model where the magnetic field curvature is simulated by a gravitational force it is shown that the stability of the compressional Alfvén wave is insensitive to the distribution function while the interacting interchange mode is sensitive. In the "local" approximation in which the curvature effects enter in a natural way it is seen that the interchange modes are insensitive so long as the anisotropy of the hot electrons is large, while other modes reflect dependence on the distribution function. Finally it is demonstrated that in the "deep well' case the results for both modes are independent of the model and of the distribution function.

I. INTRODUCTION

The potential of the ELMO Bumpy Torus (EBT) plasma confinement device[1] as a fusion reactor depends critically on the beta (ratio of plasma pressure to magnetic field pressure) value it can support since fusion power is directly proportional to this quantity. The value of such parameter is dictated by the gross stability of the system, and in recent years several investigations have been aimed at ascertaining such stability. In studying the magnetohydrodynamic (MHD) stability of EBT, it is adequate to treat the relatively cold background plasma by the fluid description, but the hot-electron component, which can provide a stabilizing effect, should be addressed by the kinetic approach. In that case the distribution function plays a critical role. In fact, conflicting results[2,3] concerning stability and the associated beta limit have emerged as to whether a delta function distribution is more or less stabilizing than a Maxwellian distribution for the hot electrons. A closely related question in this regard is whether relativistic effects also play an important role in the stability of EBT.[4,5]

It has been pointed out[6,7] that at frequencies well below the drift frequency of the hot electrons the interchange modes dominate, and as the frequencies approach the curvature drift frequency the compressional Alfvén waves and the coupled modes begin to come into play. Examination of these modes have been carried out either in the "slab" model,[2,4] where the magnetic field curvature is simulated by a gravitational force, or in a "local" model, in which the curvature effects enter in a natural way. As will be shown below, not only will the distribution function play an important role but also the model in which it is employed will. It will be seen that only in the "deep-well" approximation will the results be insensitive to both the model and the distribution function of the hot electrons.

II. ANALYSIS AND RESULTS

In this analysis short-wavelength, flute-like modes of the form $\exp[i\mathbf{k}_\perp\cdot\mathbf{r}-i\omega t]$ will be considered. For such waves the perturbed electric and magnetic fields can be expressed in terms of the scalar and vector potentials, φ and $\mathbf{A}$, as

$$\mathbf{E}' = -i\mathbf{k}_\perp\varphi + (i\omega/c)\mathbf{A}_\perp, \quad \mathbf{B}' = i\mathbf{k}_\perp\times\mathbf{A}_\perp = ik_\perp A_\perp\hat{\mathbf{b}}, \quad \hat{\mathbf{b}} = \mathbf{B}/B, \tag{1}$$

where the Coulomb gauge $\nabla\cdot\mathbf{A}=0$ has been employed. The perturbed distribution function for the hot electrons can be obtained from the relativistic Vlasov equation,[4] i.e.,

$$f' = -q\int_{-\infty}^{t}\left(\mathbf{E}'+\frac{\mathbf{v}\times\mathbf{B}'}{c}\right)\cdot\frac{\partial f^0}{\partial\mathbf{p}}\,dt' \tag{2a}$$

where $f^0(p_\perp^2, p_\parallel, \mathbf{r}_g)$ is the equilibrium distribution function expressed in terms of the constants of motion, which, in this case, are the guiding-center position $\mathbf{r}_g$ and, $p_\perp^2$ and $p_\parallel$, with

$$\mathbf{p} = m\gamma\mathbf{v}, \quad \gamma = (1+p^2/m^2c^2)^{1/2}, \tag{2b}$$

and m being the rest mass. From Eqs. (1) and (2) the perturbed distribution function can be written as

$$f' = 2m\gamma\varphi q\frac{\partial f^0}{\partial p_\perp^2} + \frac{(\hat{\mathbf{b}}\times\nabla f^0)\cdot\mathbf{A}_\perp}{cB} + iq\omega D\int_{-\infty}\left(\varphi - \frac{\mathbf{v}\cdot\mathbf{A}_\perp}{c}\right)dt, \tag{3}$$

where we introduce

$$D = 2m\gamma\frac{\partial f^0}{\partial p_\perp^2} + \frac{(\mathbf{k}_\perp\times\hat{\mathbf{b}})\cdot\nabla f^0}{m\Omega\omega},$$

and observe that the integral is to be carried out over the

 0031-9171/83/103085-07$01.90

unperturbed particle orbits. Performing such an integration leads to[4]

$$f' = 2m\gamma\varphi q\frac{\partial f^0}{\partial p_\perp^2} + \frac{(\mathbf{b}\times\nabla f^0)\cdot\mathbf{A}_\perp}{cB} + q\omega D\left(\varphi\sum_l\sum_n \frac{J_n(k_\perp\rho)J_l(k_\perp\rho)e^{i(n-l)(\alpha+\psi)}}{\omega_d-\omega+n\Omega/\gamma} - \frac{iv_\perp A_\perp}{c}\sum_l\sum_n\frac{J_n' J_l e^{i(n-l)(\alpha+\psi)}}{\omega_d-\omega+n\Omega/\gamma}\right), \tag{4}$$

where q is the particle charge, ρ is its Larmor radius, ω_d is the particle drift frequency due to the magnetic field gradient and curvature to be defined later, and α and ψ are phase angles. The dispersion relation is then obtained by using the quasineutrality condition:

$$\sum_s\int d^3p\, q_s f'^s = \sum_s q_s^2\int d^3p\left[2m\gamma\frac{\partial f^{0s}}{\partial p_\perp^2} - \omega D\sum_n\frac{1+n\mathbf{k}_\perp\times\hat{\mathbf{b}}\cdot\nabla\ln N/k_\perp^2}{\omega-\omega_{ds}-n\Omega_s/\gamma}\times\left(J_n^2\varphi - \frac{iv_\perp A_\perp}{c}J_nJ_n'\right)\right]=0, \tag{5}$$

and the perpendicular component of Ampere's law, namely

$$k_\perp^2 A_\perp = \frac{\mu_0}{c}\mathbf{k}_\perp\times\mathbf{J}\cdot\hat{\mathbf{b}} = \frac{\mu_0}{c}\sum_s q_s^2\int d^3p\, k_\perp v_\perp\omega D\times\sum_n\left(\frac{1+n\mathbf{k}_\perp\times\hat{\mathbf{b}}\cdot\nabla\ln N/k_\perp^2}{\omega-\omega_{ds}-n\Omega_s/\gamma}\right)\times\left(iJ_nJ_n'\varphi - \frac{v_\perp A_\perp}{c}J_n'^2\right), \tag{6}$$

where the first summation is over the species. It might be noted at this point that the term

$$n\mathbf{k}_\perp\times\hat{\mathbf{b}}\cdot\nabla\ln N/k_\perp^2,$$

which reflects the difference between the actual position and the guiding-center position of the particle, is generally ignored at low frequencies, but can become important for the high-frequency modes.[8] A nonrelativistic, isotropic Maxwellian distribution is chosen for the bulk species, and due to their generally low temperature, the condition $\omega\gg\omega_{di,e}$ is also assumed. Since for the modes of interest the frequency ω is comparable to the ion gyrofrequency Ω_i, but much smaller than Ω_e, it is sufficient to retain the $n=0,\ \pm1$ terms for the ions and the $n=0$ terms for the background and hot electrons. Moreover, if the guiding-center approximation, $k_\perp\rho\ll1$, is also invoked for all the species then Eqs. (5) and (6) can be put in the form

$$\sum_s\int d^3p\, q_s f'^s = -\frac{Nq^2}{T_i}\varphi\left[(\omega_{*i}-\omega_{di})\left(\frac{\omega_{di}(1+\tau_e)}{\omega^2}+\frac{\delta}{\omega}\right) - \frac{\Omega_i^2 b_i}{\omega^2-\Omega_i^2} - \frac{\omega\omega_{*i}}{\omega^2-\Omega_i^2} + \frac{\delta}{\tau_h}\left(1-\int d^3p f^{0h}\frac{\omega-\omega_{*h}}{\omega-\omega_{dh}}\right)\right] - \frac{iqNk_\perp A_\perp}{B}\left[\frac{\Omega_i^2}{\omega^2-\Omega_i^2}+\frac{1}{b_i}\frac{\omega\omega_{*i}}{\omega^2-\Omega_i^2}+(1-\delta) + \delta\int d^3p f^{0h}\left(\frac{p_\perp^2}{2m\gamma T_{\perp h}}\right)\frac{\omega-\omega_{*h}}{\omega-\omega_{dh}}\right]=0, \tag{7}$$

$$\sum_s q_s\int d^3p\, k_\perp v_\perp\sin(\alpha+\psi)f'^s = \frac{icqNk_\perp^2\varphi}{B}\left[\frac{\Omega_i^2}{\omega^2-\Omega_i^2}+\frac{1}{b_i}\frac{\omega\omega_{*i}}{\omega^2-\Omega_i^2}+(1-\delta) + \delta\int d^3p f^{0h}\left(\frac{p_\perp^2}{2m\gamma T_{\perp h}}\right)\frac{\omega-\omega_{*h}}{\omega-\omega_{dh}}\right] + \frac{ck_\perp^3 A_\perp}{\mu_0}\times\left[\beta_i\left(1+\frac{1}{2b_i}\frac{\omega^2}{\omega^2-\Omega_i^2}+\frac{1}{2b_i^2\Omega_i^2}\frac{\omega^3\omega_{*i}}{\omega^2-\Omega_i^2}\right) + \beta_e+\frac{\beta_h}{2}\int d^3p f^{0h}\left(\frac{p_\perp^2}{2m\gamma T_{\perp h}}\right)^2\frac{\omega-\omega_{*h}}{\omega-\omega_{dh}}\right] = -\frac{ck_\perp^3 A_\perp}{\mu_0}, \tag{8}$$

where

$$\tau_s = T_s/T_i,\quad b_i = k_\perp^2 T_i/m_i\Omega_i^2,\quad \delta = N_h/N_i,$$
$$\omega_{*s} = (T_{\perp s}/m\Omega)\mathbf{k}_\perp\times\hat{\mathbf{b}}\cdot\nabla\ln N_s,$$
$$\omega_{di,e} = -(\beta_t/2)\omega_{*i,e} + (2T_{i,e}/m\Omega)\mathbf{k}_\perp\cdot(\hat{\mathbf{b}}\times\hat{\mathbf{b}}\cdot\nabla\hat{\mathbf{b}}),$$
$$\beta_t = \beta_i+\beta_e+\beta_h,\quad \beta_s = \mu_0 N_s T_s/B^2.$$

From the above equation a set of algebraic equations for the vector and scalar potentials can be generated, namely

$$D_{es}\varphi + \frac{iA_\perp}{c}\left(\frac{k_\perp T_i}{m_i\Omega_i}\right)D_{ct}=0,$$
$$\frac{\mu_0 Nq^2}{c}\frac{i\varphi D_{ct}}{m_i\Omega_i} + k_\perp A_\perp D_{em}=0,$$

which in turn give rise to the dispersion equation of interest, i.e.,

$$D_{es}D_{em} + (\beta_i/2)D_{ct}^2 = 0. \tag{9}$$

In the above equations the following expressions have been introduced:

$$D_{es} = (\omega_{*i}-\omega_{di})\left(\frac{\omega_{di}(1+\tau_e)}{\omega^2}+\frac{\delta}{\omega}\right) - \frac{\Omega_i^2 b_i}{\omega^2-\Omega_i^2} - \frac{\omega\omega_{*i}}{\omega^2-\Omega_i^2} + \frac{\delta}{\tau_h}\left(1-\int d^3p f^h\frac{\omega-\omega_{*h}}{\omega-\omega_{dh}}\right),$$

$$D_{em} = 1+\beta_i\left(1+\frac{1}{2b_i}\frac{\omega^2}{\omega^2-\Omega_i^2}+\frac{1}{2b_i^2\Omega_i^2}\frac{\omega^3\omega_{*i}}{\omega^2-\Omega_i^2}\right) + \beta_e+\frac{\beta_h}{2}\int d^3p f^h\left(\frac{p_\perp^2}{2m\gamma T_{\perp h}}\right)^2\frac{\omega-\omega_{*h}}{\omega-\omega_{dh}},$$

$$D_{ct} = \frac{\Omega_i^2}{\omega^2-\Omega_i^2}+\frac{1}{b_i}\frac{\omega\omega_{*i}}{\omega^2-\Omega_i^2}+(1-\delta) + \delta\int d^3p f^h\left(\frac{p_\perp^2}{2m\gamma T_{\perp h}}\right)\frac{\omega-\omega_{*h}}{\omega-\omega_{dh}}.$$

For the modes of interest, the compressional Alfvén wave is magnetic, and the results for it can be obtained approximately by setting $D_{em}=0$. Although the interacting interchange is not magnetic it has been shown,[2,6] using the full dispersion relation, that the stability boundary for this mode can nevertheless be given approximately by $D_{em}=0$. Therefore for analytical purposes we will examine the influence of the hot-electron distribution using $D_{em}=0$, while the full dispersion relation will be used to generate the numerical results to be discussed later:

$$1+\beta_i\left(1+\frac{1}{2b_i}\frac{\omega^2}{\omega^2-\Omega_i^2}+\frac{1}{2b_i^2\Omega_i^2}\frac{\omega^3\omega_{*i}}{\omega^2-\Omega_i^2}\right)+\beta_e+\frac{\beta_h}{2}C^h=0, \tag{10}$$

where

$$C^h=\int d^3p f^h\left(\frac{p_\perp^2}{2m\gamma T_{\perp h}}\right)^2\frac{\omega-\omega_{*h}}{\omega-\omega_{dh}}.$$

It can readily be seen from Eq. (10) that the dependence on the hot-electron distribution function appears in the last term, specifically C^h, and as a result it becomes the focal point of the analysis.

If the usual assumption that the temperature of an EBT plasma is considered constant, and the density profile of all species is taken to be the same, then we can simply write

$$\omega_{dh}=\omega_{bh}+\omega_{cv_{\perp h}}+\omega_{cv_{\|h}},$$

where

$$\omega_{bh}=-\frac{\beta_t}{2}\left(\frac{p_\perp^2}{2m\gamma T_{\perp h}}\right)\omega_{*h},$$

and $\omega_{cv_{\perp h}}$ and $\omega_{cv_{\|h}}$ combined represent the drift due to the magnetic curvature. It should be noted at this point that ω_{bh} and $\omega_{cv_{\perp h}}$ together constitute the familiar ∇B drift. The use of the individual $\omega_{cv_{\perp h}}$ and $\omega_{cv_{\|h}}$ is for convenience and their definitions depend on the model used to examine the problem.

A. The slab model[2-4]

In this model the magnetic field lines are assumed to be straight, say in the z direction, with the curvature simulated by a gravitational force in the x direction which is the same direction as that of the density gradient. In that case the curvature drift frequencies become

$$\omega_{cv_{\perp h}}=\bar{\omega}_{cv_{\perp h}}=kT_{\perp h}\sigma/m\Omega R_c,\quad \sigma=1+\tfrac{1}{2}(\beta_{\perp h}-\beta_{\|h}),$$
$$\omega_{cv_{\|h}}=\bar{\omega}_{cv_{\|h}}=kT_{\|h}/m\Omega R_c,\quad k=\mathbf{k}_\perp\cdot\hat{\mathbf{y}}. \tag{11}$$

It may readily be noted that modes that satisfy the condition

$$\omega-(\omega_{cv_{\perp h}}+\omega_{cv_{\|h}})\simeq 0,$$

such as the compressional Alfvén waves,[4] are independent of the hot-electron distribution function since for these modes

$$C^h\simeq-\frac{\omega-\omega_{*h}}{\bar{\omega}_{bh}}\int d^3p_\perp f^h\left(\frac{p_\perp^2}{2m\gamma T_{\perp h}}\right)=\frac{\omega_{*h}-\omega}{\bar{\omega}_{bh}} \tag{12}$$

is a constant regardless of the distribution function provided, however, that it satisfied the ideal gas law. Moreover, it is equally evident that for modes for which

$$\omega-(\omega_{cv_{\perp h}}+\omega_{cv_{\|h}})\neq 0,$$

such as the interacting interchange mode[2,4] (where $\omega\ll\omega_{cvh}$), the stability boundary is sensitive to the form of the hot-electron distribution function, except when the deep magnetic well condition is invoked; a case which will be examined shortly. Finally, it should be noted that the bar over the frequcncies appearing in Eqs. (11) and (12) denote evaluation at thermal energies.

B. The "local" model[3,5,6]

In this model the field curvature enters in a natural way. Unlike the slab model, the field lines are allowed to bend and, for the cases of interest modes that are localized in regions of bad curvature, are considered. Accordingly, the curvature drift frequencies become

$$\omega_{cv_{\perp h}}=\frac{k\sigma}{m\Omega R_c}\left(\frac{p_\perp^2}{2m\gamma}\right),$$
$$\omega_{cv_{\|h}}=\frac{k}{m\Omega R_c}\left(\frac{p_\|^2}{m\gamma}\right),\quad k=\mathbf{k}_\perp\cdot\hat{\boldsymbol{\theta}}, \tag{13a}$$

where $\hat{\boldsymbol{\theta}}$ is a unit vector in the poloidal direction. In view of this we can write

$$\omega_{dh}=\frac{p_\perp^2}{2m\gamma}\frac{k}{m\Omega}\left(-\frac{\beta_t}{2\Delta}+\frac{\sigma}{R_c}\right)+\frac{k}{m\Omega R_c}\left(\frac{p_\|^2}{m\gamma}\right), \tag{13b}$$

where

$$\Delta^{-1}=|\nabla\ln N|$$

is the half-width of the hot-electron ring. When the temperature anisotropy $(T_{\perp h}/T_{\|h})$ is large as expected for the hot electrons in EBT, then C^h of Eq. (10) can be approximated by

$$C^h\simeq\frac{1}{T_{\perp h}^2}\int d^3p f^h\left(\frac{p_\perp^2}{2m\gamma}\right)^2\frac{\omega-\omega_{*h}}{\tilde{\omega}}\times\left[1+\frac{\omega_{cv_{\|h}}}{\tilde{\omega}}+\left(\frac{\omega_{cv_{\|h}}}{\tilde{\omega}}\right)^2+\cdots\right], \tag{14}$$

where

$$\tilde{\omega}=\omega-\omega_{bh}-\omega_{cv_{\perp h}}=\omega-(\bar{\omega}_{bh}+\bar{\omega}_{cv_{\perp h}})(p_\perp^2/2m\gamma T_{\perp h}),$$
$$\omega_{cv_{\|h}}=\bar{\omega}_{cv_{\|h}}(p_\|^2/m\gamma T_{\|h}).$$

If, in addition to neglecting terms of order $(T_{\|h}/T_{\perp h})^2$, we consider modes with

$$\omega\ll\omega_{cvh},\omega_{bh},\omega_{*h},$$

as in the interacting interchange mode, then Eq. (14) may be expressed as

$$C^h=\frac{\omega_{*h}}{\bar{\omega}_{bh}+\bar{\omega}_{cv_{\perp h}}}\int d^3p f^h\times\left(\frac{p_\perp^2}{2m\gamma T_{\perp h}}-\frac{\bar{\omega}_{cv_{\|h}}}{\bar{\omega}_{bh}+\bar{\omega}_{cv_{\perp h}}}\frac{p_\|^2}{m\gamma T_{\|h}}\right)=\frac{\omega_{*h}}{\bar{\omega}_{bh}+\bar{\omega}_{cv_{\perp h}}}\left(1-\frac{\bar{\omega}_{cv_{\|h}}}{\bar{\omega}_{bh}+\bar{\omega}_{cv_{\perp h}}}\right), \tag{15}$$

which is clearly independent of the distribution function. It should be kept in mind that the above result is valid for low frequencies and as long as terms of order $(T_{\|h}/T_{\perp h})^2$ or higher can be neglected. Since the next-order (NO) correction term to the above equation is

$$C^h_{\rm NO} = \frac{\omega_{*h}\,\bar{\omega}^2_{cv_{\|h}}}{(\bar{\omega}_{bh}+\bar{\omega}_{cv_{\perp h}})^3}\int d^3p f^h \frac{(p_\|^2/m\gamma T_{\|h})^2}{p_\perp^2/2m\gamma T_{\perp h}}, \tag{16}$$

it is clear that this term reflects sensitive dependence on the hot-electron distribution function.

For modes for which the frequency ω cannot be neglected in comparison with the hot-electron drift frequency, as in the compressional Alfvén waves case, the quantity C^h can be expanded to read (with $T_{\|h}=0$)

$$\begin{aligned} C^h &= -\frac{\omega-\omega_{*h}}{\bar{\omega}_{dh}}\int d^3p f^h\left[\frac{p_\perp^2}{2m\gamma T_{\perp h}}+\frac{\omega}{\bar{\omega}_{dh}}\right. \\ &\quad \left.+\left(\frac{\omega}{\bar{\omega}_{dh}}\right)^2\frac{1}{p_\perp^2/2m\gamma T_{\perp h}}+\cdots\right] \\ &= -\frac{\omega-\omega_{*h}}{\bar{\omega}_{dh}}\left[1+\frac{\omega}{\bar{\omega}_{dh}}\right. \\ &\quad \left.+\left(\frac{\omega}{\bar{\omega}_{dh}}\right)^2\int d^3p f^h\left(\frac{p_\perp^2}{2m\gamma T_{\perp h}}\right)^{-1}+\cdots\right], \end{aligned} \tag{17}$$

which clearly reveals dependence on the distribution function unless terms of order $(\omega/\bar{\omega}_{dh})^2$ or higher can be neglected.

We conclude this section by noting that, in the local model, modes for which $\omega \ll \omega_{\rm dh}$ are insensitive to the distribution function as long as the anisotropy is large; and that modes for which $\omega \simeq \omega_{dh}$ show dependence on it.

C. The "deep-well" approximation[5]

Since stabilization of the interchange modes occurs as a result of the magnetic "well" which the hot electrons dig, it is often convenient to invoke the "deep-well" approximation in the stability analysis. Such a condition is given by

$$\beta_h/2\Delta \gg (\sigma + T_{\|h}/T_{\perp h})/R_c,$$

and, as we shall shortly demonstrate, the stability boundary for modes with $\omega \lesssim \omega_{cv_{\|h}} + \omega_{cv_{\perp h}}$ is insensitive not only to the distribution function but also to the models discussed above. To see this we follow Ref. 5 and carry out the following expansion:

$$\frac{1}{\omega-\omega_{bh}-\omega_{cv_{\perp h}}-\omega_{cv_{\|h}}} \simeq -\frac{1}{\omega_{bh}}\left(1-\frac{\omega_{cv_{\perp h}}+\omega_{cv_{\|h}}-\omega}{\omega_{bh}}\right), \tag{18}$$

and, since in the slab model

$$\omega_{cv_{\perp h}} = \bar{\omega}_{cv_{\perp h}}, \quad \omega_{cv_{\|h}} = \bar{\omega}_{cv_{\|h}},$$

the quantity C^h becomes in this case

$$\begin{aligned} C^h &= \frac{\omega_{*h}-\omega}{\bar{\omega}_{bh}}\int d^3p f^h\left(\frac{p_\perp^2}{2m\gamma T_{\perp h}}+\frac{\omega-\bar{\omega}_{cv_{\perp h}}-\bar{\omega}_{cv_{\|h}}}{\bar{\omega}_{bh}}\right) \\ &= \frac{\omega_{*h}-\omega}{\bar{\omega}_{bh}}\left(1+\frac{\omega-\bar{\omega}_{cv_{\perp h}}-\bar{\omega}_{cv_{\|h}}}{\bar{\omega}_{bh}}\right). \end{aligned} \tag{19}$$

If we do the same thing in the local model, the result would be

$$\begin{aligned} C^h &= \frac{\omega_{*h}-\omega}{\bar{\omega}_{bh}}\left[\left(1-\frac{\bar{\omega}_{cv_{\perp h}}}{\bar{\omega}_{bh}}\right)\int d^3p f^h\frac{p_\perp^2}{2m\gamma T_{\perp h}}\right. \\ &\quad \left.-\frac{\bar{\omega}_{cv_{\|h}}}{\bar{\omega}_{bh}}\int d^3p f^h\frac{p_\|^2}{m\gamma T_{\|h}}+\frac{\omega}{\bar{\omega}_{bh}}\int d^3p f^h\right] \\ &= \frac{\omega_{*h}-\omega}{\bar{\omega}_{bh}}\left(1+\frac{\omega-\bar{\omega}_{cv_{\perp h}}-\bar{\omega}_{cv_{\|h}}}{\bar{\omega}_{bh}}\right), \end{aligned} \tag{20}$$

which we readily note to be identical with (19) thereby validating the assertion that in the deep-well case the results are independent of the model and of the distribution function. If, for example, we use the parameters employed by Nelson[2] in his slab model analysis, namely

$$T_{\|h}/T_{\perp h} = 1, \quad \Delta/R_c = 0.1, \quad \beta_h = 1,$$

then it is clear that the deep-well approximation

$$(1+T_{\|h}/T_{\perp h})(2\Delta/\beta_h R_c) = 0.4$$

is not satisfied even for $\beta_h = 1$, and as a consequence his delta function and Maxwellian distributions do indeed give rise to different results.

It is perhaps useful at this junction to provide some physical insight regarding the sensitivity (or lack of it) of the results to the distribution function in the various models discussed above. These effects can be traced back to the mechanisms that give rise to the various instabilities which we will now attempt to analyze using the single-particle picture. For this purpose we recall from Eq. (13b) those portions of the hot-electron drift velocity relevant to the mechanism of interest, namely with $(T_{\|h}=0)$

$$v_d = (p_\perp^2/4m^2\gamma\Omega\Delta)(-\beta_c + 2\Delta\sigma/R_c), \tag{21}$$

where we note that the first term represents the well dug by the background plasma, and the second represents the curvature effect (force). It is the competition between the stabilizing effect of the curvature and the destabilizing effect of the background plasma well that leads to the instability of the interacting interchange mode. In the local model, Eq. (21) remains valid and for stability we require

$$\beta_c < 2\Delta\sigma/R_c$$

for all distributions since in this case all the particles move in one direction. In the slab model, however, Eq. (21) is replaced by

$$v_d = \frac{p_\perp^2}{2m^2\gamma\Omega}\left(-\frac{\beta_c}{2\Delta}\right)+\frac{\sigma T_{\perp h}}{m\Omega R_c},$$

where it is seen that the hot electrons feel the same stabilizing effect due to curvature $(\sim T_{\perp h})$ while they experience different effects due to the driving force $(\sim p_\perp^2)$. As a result the stability boundary would indeed be sensitive to the distribution function as indicated earlier. This is borne out in the results of Refs. 2 and 4. It is also clear why such analysis also reflects the relativistic effects brought forth in Ref. 4. One can repeat the same argument to explain the sensitivity, or lack of it, of the other modes examined earlier as well as the cases when $T_{\|h}$ is included.

We conclude this section by remarking that the local model is physically more meaningful since in this model the curvature effect enters in a natural way from the equations of motion and pressure balance, while in the slab model this effect is simulated by a gravitational force resulting in the loss of many details, particularly when kinetic theory is employed.

III. NUMERICAL RESULTS

In an effort to corroborate the above conclusions, we have chosen to generate stability results for the following hot-electron distribution functions using the full dispersion equation [Eq. (9)] in the local model:

$$f^{h1}=\frac{|v_\parallel|}{\pi m^3}\delta\left(v_\parallel^2-\frac{T_{\parallel h}}{m}\right)\delta\left(v_\perp^2-\frac{2T_{\perp h}}{m}\right),\quad \gamma\simeq 1.$$

This distribution yields for the relevant integrals in C^h the quantities

$$\begin{aligned}
&\int d^3p f^h\frac{\omega-\omega_{*h}}{\omega-\omega_{dh}}=\frac{\omega-\omega_{*h}}{\omega-\bar\omega_{dh}},\\
&\int d^3p f^h\left(\frac{p_\perp^2}{2m\gamma T_{\perp h}}\right)\frac{\omega-\omega_{*h}}{\omega-\omega_{dh}}=\frac{\omega-\omega_{*h}}{\omega-\bar\omega_{dh}},\\
&\int d^3p f^h\left(\frac{p_\perp^2}{2m\gamma T_{\perp h}}\right)^2\frac{\omega-\omega_{*h}}{\omega-\omega_{dh}}=\frac{\omega-\omega_{*h}}{\omega-\bar\omega_{dh}}.
\end{aligned}\tag{22}$$

The second distribution function is of the form

$$f^{h2}=\frac{|v_\parallel|}{2\pi m^2 T_{\perp h}}\delta\left(v_\parallel^2-\frac{T_{\parallel h}}{m}\right)\exp\left(-\frac{mv_\perp^2}{2T_{\perp h}}\right),\quad \gamma\simeq 1;$$

which in turn gives

$$\int d^3p f^h\frac{\omega-\omega_{*h}}{\omega-\omega_{dh}}=\frac{\omega-\omega_{*h}}{\bar\omega_{bh}+\bar\omega_{cv_{\perp h}}}e^{-a}E_i(a),$$

$$\begin{aligned}
&\int d^3p f^h\left(\frac{p_\perp^2}{2m\gamma T_{\perp h}}\right)\frac{\omega-\omega_{*h}}{\omega-\omega_{dh}}\\
&\quad=\frac{\omega-\omega_{*h}}{\bar\omega_{bh}+\bar\omega_{cv_{\perp h}}}[1-ae^{-a}E_i(a)],
\end{aligned}\tag{23}$$

$$\begin{aligned}
&\int d^3p f^h\left(\frac{p_\perp^2}{2m\gamma T_{\perp h}}\right)^2\frac{\omega-\omega_{*h}}{\omega-\omega_{dh}}\\
&\quad=-\frac{\omega-\omega_{*h}}{\bar\omega_{bh}+\bar\omega_{cv_{\perp h}}}[1+a-a^2e^{-a}E_i(a)],
\end{aligned}$$

where $a=[\omega-\bar\omega_{cv_{\parallel h}}]/[\bar\omega_{bh}+\bar\omega_{cv_{\perp h}}]$ and $E_i(a)$ is the familiar exponential integral. For the third distribution function we choose

$$f^{h3}=\left(\frac{\theta}{8\pi}\right)^{1/2}\frac{e^{-\theta\gamma}}{m^2c^2K_{3/2}(\theta)}\delta(p_\parallel),$$

where

$$\theta=mc^2/T_{\perp h},\quad \gamma=(1+p_\perp^2/m^2c^2)^{1/2},$$

and $K_{3/2}(\theta)$ is the modified Bessel function. This distribution function represents a highly anisotropic, relativistic hot-electron species for which it can be shown that[4]

$$\begin{aligned}
&\int d^3p f^h\frac{\omega-\omega_{*h}}{\omega-\omega_{dh}}=-\frac{2(\omega-\omega_{*h})}{\bar\omega_{bh}+\bar\omega_{cv_{\perp h}}}\frac{\theta}{1+\theta}\\
&\qquad\times\left(\frac{1}{\theta}+\frac{1}{\nu-\alpha}[e^{-G}(b\alpha+1)E_i(G)\right.\\
&\qquad\left.-e^{-H}(b\nu+1)E_i(H)]\right)\\
&\int d^3p f^h\left(\frac{p_\perp^2}{2m\gamma T_{\perp h}}\right)\frac{\omega-\omega_{*h}}{\omega-\omega_{dh}}\\
&\quad=\frac{\omega-\omega_{*h}}{\bar\omega_{bh}+\bar\omega_{cv_{\perp h}}}\frac{\theta^2}{1+\theta}\left(\frac{1+b}{\theta}+\frac{1}{\theta^2}\right.\\
&\qquad+\frac{1}{\nu-\alpha}[e^{-G}(b^2\alpha+b)E_i(G)\\
&\qquad\left.-e^{-H}(b^2\nu+b)E_i(H)]\right),
\end{aligned}\tag{24}$$

$$\begin{aligned}
&\int d^3p f^h\left(\frac{p_\perp^2}{2m\gamma T_{\perp h}}\right)^2\frac{\omega-\omega_{*h}}{\omega-\omega_{dh}}\\
&\quad=-\frac{1}{2}\frac{\omega-\omega_{*h}}{\bar\omega_{bh}+\bar\omega_{cv_{\perp h}}}\frac{\theta^3}{1+\theta}\\
&\qquad\times\left(\frac{b(1+b)}{\theta}+\frac{2+b}{\theta^2}+\frac{2}{\theta^3}+\frac{1}{\nu-\alpha}\right.\\
&\qquad\left.\times[e^{-G}(b^3\alpha+b^2)E_i(G)-e^{-H}(b^3\gamma+b^2)E_i(H)]\right),
\end{aligned}$$

where

$$b=(2/\theta)\omega/(\bar\omega_{bh}+\bar\omega_{cv_{\perp h}}),\quad \alpha=(b/2)-\tfrac{1}{2}(b^2+4)^{1/2},$$
$$\nu=b/2+(b^2+4)^{1/2},\quad G=\theta(\alpha-1),\quad H=\theta(\nu-1).$$

It might also be noted that in the nonrelativistic limit, i.e., $\theta\to\infty$, Eqs. (23) and (24) become identical when $T_{\parallel h}/T_{\perp h}$ is set equal to zero.

In order to compare the stability results associated with the above three distributions on an equal basis it is necessary to demonstrate that they all have equal pressure moments. The perpendicular pressure is given by

$$P_{\perp h}=\int nm\frac{\gamma v_\perp^2}{2}f^h 2\pi p_\perp\,dp_\perp\,dp_\parallel,\tag{25}$$

which in the case of the first distribution function f^{h1} becomes

$$P_{\perp h}=\frac{nm}{2}\int_0^\infty dv_\parallel^2\,\delta(v_\parallel^2)\int_0^\infty dv_\perp^2\,v_\perp^2\delta\left(v_\perp^2-\frac{2T_{\perp h}}{m}\right)=nT_{\perp h}.\tag{26}$$

When the second distribution function f^{h2} is used the result becomes

$$P_{\perp h}=\frac{nm^2}{4}\int_0^\infty dv_\parallel^2\,\delta(v_\parallel^2)\int_0^\infty dv_\perp^2\,v_\perp^2 e^{-mv_\perp^2/2T_{\perp h}}=nT_{\perp h},\tag{27}$$

where integration by parts has been carried out on the second integral. In contrast to the first two distribution functions, which are nonrelativistic, the third f^{h3} is relativistic, for which the perpendicular pressure can be written as[4]

$$\begin{aligned}
P_{\perp h}=&\left(\frac{\theta}{8\pi}\right)^{1/2}\frac{n}{m^2c^2K_{3/2}(\theta)}\int_{-\infty}^\infty dp_\parallel\,\delta(p_\parallel)\\
&\times\int_0^\infty 2\pi p_\perp\,dp_\perp\frac{m\gamma v_\perp^2}{2}e^{-\theta\gamma},
\end{aligned}\tag{28}$$

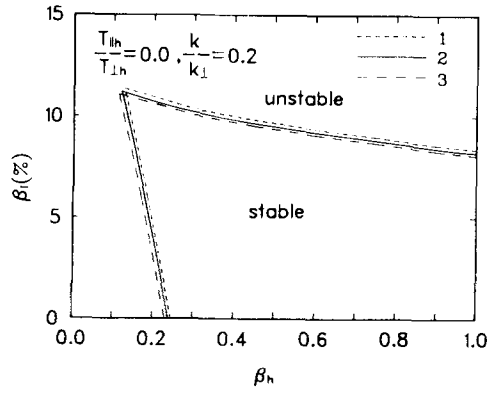

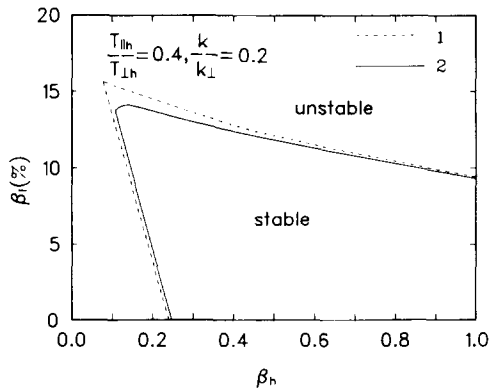

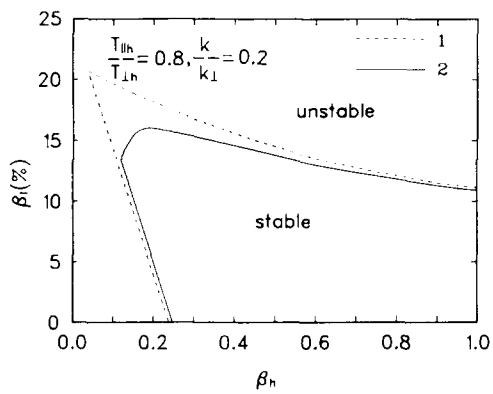

FIG. 1. Interchange mode stability boundary (a) for a highly anisotropic distribution function, (b) for a moderately anisotropic distribution function, and (c) for a nearly isotropic hot-electron distribution function.

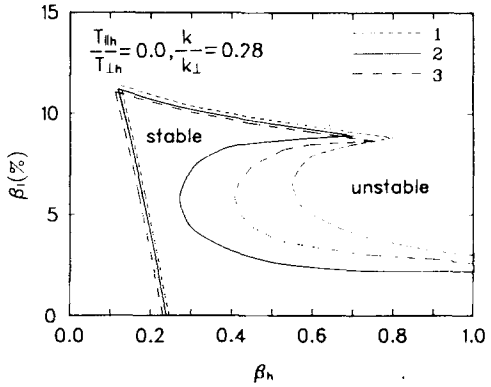

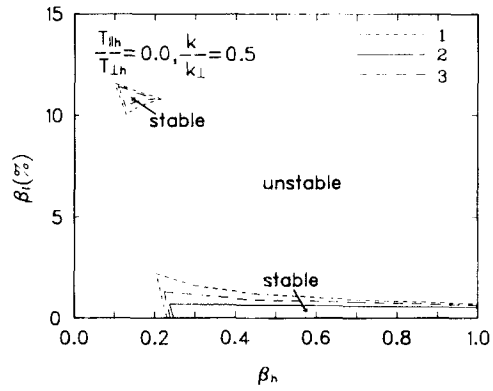

FIG. 2. Dependence of (a) compressional Alfvén wave on the distribution function and (b) compressional Alfvén wave at stronger coupling.

where γ and $\mathbf{p}$ had been defined earlier [see Eq. (2b)]. If we let $\gamma = \cosh x$ and $p_\perp = mc \sinh x$ then the last integral in the above equation assumes the form[9]

$$\int_0^\infty p_\perp \, dp_\perp m\gamma v_\perp^2 e^{-\gamma\theta} = m^3c^4 \int_0^\infty e^{-\theta\cosh x} \sinh^3 x \, dx$$

$$= \pi m^3 c^4 \left[\left(\frac{2}{\pi\theta}\right)^{3/2} K_{3/2}(\theta)\right].$$

In view of this, Eq. (28) simply becomes

$$P_{\perp h} = nmc^2/\theta = nT_{\perp h}, \tag{29}$$

and we see that all of the distributions produce the same dependence of the perpendicular pressure on $T_{\perp h}$. It should be kept in mind that agreement on $p_{\perp h}$ among the three distributions is obtained when $T_{\|h} = 0$, due to the fact that the relativistic distribution was constructed deliberately to be highly anisotropic. When $T_{\|h} \neq 0$ then agreement is obtained for distributions 1 and 2 only.

In obtaining the results shown in the figures, the following common parameters were used:

$$T_e/T_i = 0, \quad T_h/T_i = 2000, \quad k_\perp \rho_i = 0.1,$$
$$\Delta/R_c = 0.06, \quad \theta = 0.1, \quad \rho_i/\Delta = -0.06;$$

and the following definitions for the frequencies appearing in Eqs. (22)–(24) were also employed:

$$\omega_{*h} = \frac{kT_{\perp h}}{m\Omega\Delta}, \quad \bar{\omega}_{bh} = -\frac{(\beta_c + \beta_h)}{2}\frac{kT_{\perp h}}{m\Omega\Delta},$$

$$\bar{\omega}_{cv_{\perp h}} = \frac{kT_{\perp h}\sigma}{m\Omega R_c}, \quad \bar{\omega}_{cv_{\|h}} = \frac{kT_{\|h}}{m\Omega R_c}.$$

Figure 1(a) shows the upper limit on the interacting interchange mode as well as the lower limit for the background plasma interchange, and as predicted analytically earlier there is no sensitivity to the distribution function for the interacting interchange since the hot electrons in this case are extremely anisotropic (i.e., $T_{\|h}/T_{\perp h} = 0$). This figure also shows no coupling to the compressional Alfvén wave since $k/k_\perp = 0.2$ which is small. Figures 1(b) and 1(c) reveal different results as the anisotropy condition is relaxed, i.e., as

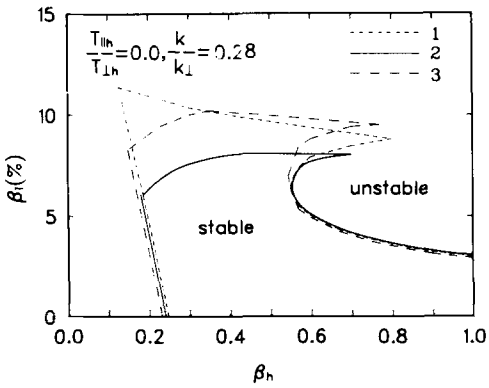

FIG. 3. Dependence of stability boundary on the hot-electron distribution function in the slab model.

$T_{\|h}/T_{\perp h}$ becomes larger (keeping in mind that the relativistic distribution is not valid for finite $T_{\|h}/T_{\perp h}$). They also show that for large β_h, the upper limit for the interacting interchange mode for distributions 1 and 2 become almost the same thus confirming the "deep-well" limit of Ref. 5. When contrasted to Fig. 1, Figs. 2(a) and 2(b) display the stronger coupling to the compressional Alfvén waves that results from increasing the value of $k_\|/k_\perp$, which in turn means a smaller angle between the direction of propagation of the Alfvén wave and the curvature drifts; a condition that belies stronger coupling. Although the upper limit on β_i for the interacting interchange is the same for all distributions, Figs. 2(a) and 2(b) show that the stability boundary for the compressional Alfvén waves is quite sensitive to the distribution function with the anisotropic Maxwellian (2) being the least stable while the delta function (1) showing the most stability. Once again, these same figures indicate that at larger β_h, corresponding to the deep-well case, the sensitivity to the distribution function practically disappears. Figure 3 has been included for purposes of comparison and it shows that in the slab model the upper limit for the interacting interchange mode is quite sensitive to the distribution function while the lower limit for the compressional Alfvén wave is not, in agreement with the earlier analytical predictions. Finally, it can be seen from Figs. 1(a) and 3 that the results for the delta function distribution is independent of the model; and in all cases the background plasma interchange is completely independent of the model and distribution functions as expected.

ACKNOWLEDGMENT

This work is supported by the U. S. Department of Energy.

[1]R. A. Dandl, H. O. Eason, P. H. Edmonds, and A. C. England, Nucl. Fusion **11**, 411 (1971).
[2]D. B. Nelson, Phys. Fluids **23**, 1850 (1980).
[3]K. T. Tsang and C. Z. Cheng, in *Proceedings of the Workshop on EBT Stability Theory*, Oak Ridge, CONF-81052 (ORNL, Oak Ridge, TN, 1981), May 1981, p. 141.
[4]K. T. Nguyen, T. Kammash, and R. Kashuba, in *Proceedings of the Workshop on Hot Electron Ring Physics*, San Diego, Dec. 1981 (ORNL, Oak Ridge, TN, 1982), CONF-811203, p. 289.
[5]H. L. Berk, J. W. VanDam, M. N. Rosenbluth, and D. A. Spong, Institute for Fusion Studies Report No. IFSR50, Austin, Dec. 1981.
[6]J. W. VanDam and Y. C. Lee, *Proceedings of the Workshop on EBT Ring Physics*, Oak Ridge, Dec. 1979 (ORNL, Oak Ridge, TN, 1979), CONF-7911228, p.471.
[7]D. A. Spong, Oak Ridge Report ORNL/TM-8021, October 1981.
[8]H. L. Berk and R. R. Dominguez, Institute for Fusion Studies Report No. IFSR70, Austin, October 1982.
[9]I. S. Gradshteyn and I. M. Ryzhik, *Table of Integrals, Series and Products* (Academic, New York, 1965).